Spatial and temporal temperature distributions in carbon nanotubes exposed to red and near-infrared laser radiation

D. Boldor[a], A.S. Biris[b], W.T. Monroe[a]

[a]Department of Biological and Agricultural Engineering, Louisiana State University Agricultural Center
[b]Nanotechnology Center, Applied Science Dept., University of Arkansas at Little Rock.

Introduction

Carbon nanotubes are impressive structures of small size and unique electrical properties, extremely attractive for a variety of applications in science and engineering. One potential application of considerable interest is their use in cancer treatment, due to their high absorbance in the near infrared spectrum, in which biological tissues do not absorb very well.[1,2] Hyperthermia treatment of cancer cells with other nanoparticles (i.e. gold) has been demonstrated, too, [2,3] but usually their peak absorbance is in a less favorable visible spectrum.[4,5] Several disadvantages of current temperature measurement methods include trade-offs between fragility and temporal response, inconsistencies of thermal properties between the probe tip and the sample being measured, and single point measurements, not ideal for measuring samples that contain high temperature gradients.[6] The authors propose to use infrared thermography, to overcome these disadvantages. The information can be used in estimating dose-response calibration curves for selective hyperthermia of cancer and other cells.

Experimental

MWCNTs Synthesis. MWCNTs (multiwall carbon nanotubes) were prepared by Radio-Frequency CVD on a Fe-Co/$CaCO_3$ (2.5:2.5/95 wt.%) catalyst with acetylene as the carbon source as described before.[7]

Micro-Thermography of MWCNTs exposed to650 nm. A small brass metal stage on adjustable platform was used for positioning and focusing in on the samples, which were loaded in d=0.3cm punched holes (Fig. 1). Samples were targeted with up to four 650nm red lasers (2.5mW power, #90725, Cen-Tech, Camarillio, CA), power density of 0.026 W/cm^2 (as measured with Power Meter, #1815-C, Newport Corp., Irvine, CA).

Thermal images were acquired at 1 Hz using a SC500 Thermacam (FLIR Systems, Boston, MA), with micro lenses with a field of view of 4x6 mm (max. resolution of 18μm/pixel). Lasers were activated sequentially at 1min intervals. Data analysis was performed by embedding Thermacam Researcher sessions into Microsoft Excel. All tests were performed in triplicate.

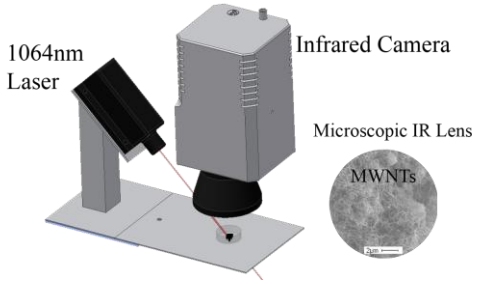

Fig. 1. Schematic of experimental setup. Only one laser is shown, but for the 650 nm tests the 4 lasers were symmetrically placed on all sides of the target area.

Thermography of MWCNTs exposed to 1064 nm. The sample and the laser (DP-1064-1000K, Lasermate Group, Pomona, CA) were positioned and aligned inside a shielding chamber (Fig. 1). The laser's (15.5 cm from the sample, 45° angle, Gaussian beam distribution with a $1/e^2$ = 2 mm), max power density used was 12.412 W/cm^2 (at 390 mW). Weighed samples were positioned on a polycarbonate platform in the beam path and treated at five different power levels (53mW, 130mW, 231mW, 320mW, and 390mW) for 30 second intervals. Thermal images were acquired and processed as described above except that they were recorded on a FLIR A40 infrared camera without the microscopic lens. Graphite (Pentel of America Inc., Torrance, CA) was used in parallel as a control to demonstrated the better electron-phonon interaction of CNTs vs. graphene.[35] All tests were performed in triplicate.

Results and Discussions

MWCNTs treated with 650 nm laser irradiation showed a modest 6-7°C increase over the graphite control and a 10°C increase over baseline (Fig. 2), both of them clearly visible in the IR images (Fig. 3, left) even at the low 10mW power used. Maximum temperature follows a linear relationship with the power level of the laser used. MWCNTs treated with the higher power 1064 nm laser showed a much larger increase in temperatures. During the 390mW treatments, the target areas maximum temperature reached at or above the 265°C limit of the camera's normal recording range (Fig 3, right), compared to compared to only 160°C for

graphite. The temperature also follows a linear increase with temperature, but for MWNTs linearity is more difficult to infer due to the saturation of camera sensor at the high temperatures (Fig. 4).

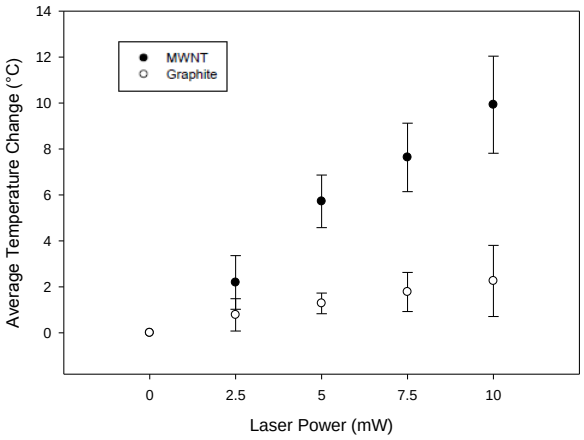

Fig. 2. Average maximum temperature increase above baseline of MWNTs and graphite vs. power while being treated with four 650 nm-2.5 mW laser sources in succession (mean ± std).

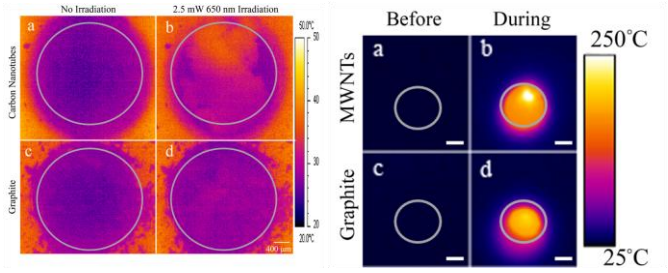

Fig. 3. Infrared images before (a,c) and during laser treatment (b,d) with four 650nm-2.5mW lasers (left) and a 1064nm - 320 mW laser (right). Images are of MWNTs (a,b) and graphite (c,d); target area inside circle (scale bars in the lower right corners of right image are 4 mm). MWNT temperatures exceeded the 265°C limit for the normal range of the infrared camera

The average target temperatures were also significantly higher for MWCNTs than for graphite (**Fig. 4**), with the linear variation with power clear for both sample and control. The observed kinetics of laser absorption (response time of less than 1 seconds) is ideal for photothermal ablation applications due to its high photon-electron-phonon interaction in the MWCNTs during the laser irradiation compared to other types of electromagnetic energy excitation.

Thermal properties of CNTs strongly depend on the phonon dispersion relations and the phonon density of states, since for 3D crystalline graphite and 2D graphene layers, from which CNTs are derived, the dominant contribution to the heat capacity comes from the phonons, while the electronic contribution can be neglected.[8] Each CNT is excited to the electronic excited state, followed by a rapid relaxation to ground state with an effective electron-phonon conversion of the absorbed photon energy into heat. Because of the very fast heat diffusion time, thermal energy rapidly diffuses along the CNT wall and then to the inside and outside medium. The infrared images of MWNTs and graphite reveal the spatial heating patterns (**Fig. 3**), which is an important advantage for the method, in addition to its speed, lack of interference with laser absorption, repeatability, and its remote nature which prevents interference with the phenomena observed.

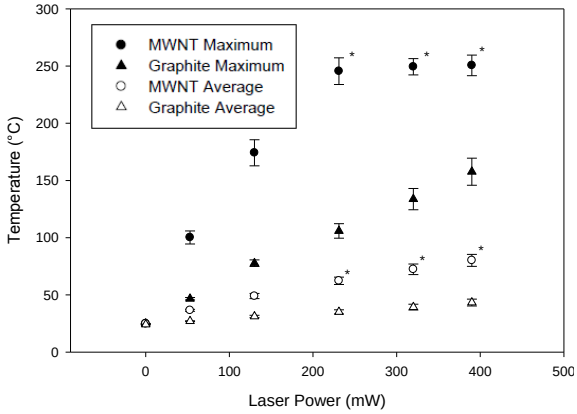

Fig. 4. Maximum and average temperatures as a function of laser power level. *Actual temperatures above detection limit of 265°C

Conclusion

This study demonstrated IR thermography is an appropriate tool for measuring temperature changes in bulk CNT samples during laser treatment at both low and high laser powers. The method showed advantages over the traditional measurement techniques and was able to identify and quantify temperature maximums not previously reported, which should be biologically significant for targeted hyperthermia of cancer and other cells. The results demonstrated here suggest that a tolerable dosage of CNTs may be sufficient to act as efficient agents of photothermal therapy.

Acknowledgements: This manuscript was published with the approval of the Director of the Louisiana AES as publication #2009-232-3882.

References

1. Kam, N. W.; O'Connell, M.; Wisdom, J. A.; Dai, H. *Proc. Natl. Acad. Sci. U.S.A.* 2005, *102*, 11600.
2. Endo, M.; Iijima, S.; Dresselhaus, M. *Carbon Nanotubes*; Elsevier Science Limited, 1996.
3. O'Neal, D. P.; Hirsch, L. R.; Halas, N. J.; Payne, J. D.; West, J. L. *Cancer Lett.* 2004, *209*, 171.
4. Zharov, V. P.; Mercer, K. E.; Galitovskaya, E. N.; Smeltzer, M. S. *Biophys. J.* 2006, *90*, 619.
5. El-Sayed, I. H.; Huang, X.; El-Sayed, M. A. *Cancer Lett.* 2006, *239*, 129.
6. Choi, B.; Pearce, J. A.; Welch, A. J. *Phys. Med. Biol.* 2000, *45*, 541.
7. Boldor, D., N.M. Gerbo, W.T. Monroe, J.H. Palmer, Z. Li, A.S. Biris 2008. *Chem Mat* 20(12): 4011-4016.
8. Dresselhaus, M. S.; Eklund, P.C. *Adv. Phys.* 2000, *49*, 705.